

Branching annihilating random walks with long-range attraction in one dimension

Su-Chan Park (박수찬)

Department of Physics, The Catholic University of Korea, Bucheon 14662, Republic of Korea

(Dated: May 21, 2020)

We introduce and numerically study the branching annihilating random walks with long-range attraction (BAWL). The long-range attraction makes hopping biased in such a manner that particle's hopping along the direction to the nearest particle has larger transition rate than hopping against the direction. Still, unlike the Lévy flight, a particle only hops to one of its nearest-neighbor sites. The strength of bias takes the form $x^{-\sigma}$ with non-negative σ , where x is the distance to the nearest particle from a particle to hop. By extensive Monte Carlo simulations, we show that the critical decay exponent δ varies continuously with σ up to $\sigma = 1$ and δ is the same as the critical decay exponent of the directed Ising (DI) universality class for $\sigma \geq 1$. Investigating the behavior of the density in the absorbing phase, we argue that $\sigma = 1$ is indeed the threshold that separates the DI and non-DI critical behavior. We also show by Monte Carlo simulations that branching bias with symmetric hopping exhibits the same critical behavior as the BAWL.

I. INTRODUCTION

The branching annihilating random-walks model (BAW) [1] is a reaction-diffusion system with pair annihilation [$2A \rightarrow 0$] and branching m offspring by a particle [$A \rightarrow (m+1)A$] as well as (symmetric) diffusion. The competition between pair annihilation and branching can bring about an absorbing phase transition between an active phase with nonzero steady-state density and an absorbing phase with zero steady-state density. The BAW exhibits rich phenomena in that critical behavior depends on the parity of the number m of offspring [1–4]. It belongs to the directed percolation (DP) universality class [5–9] for odd m , whereas it belongs to the directed Ising (DI) universality class [10–16] for even m . For a review of these two classes, see, e.g., Refs. [17–19]

When a global hopping bias is introduced to the BAW in such a way that hopping along a predefined direction is preferred (for example, in one dimension hopping to the right has larger transition rate than hopping to the left), this bias in the (asymptotic) field theory is gauged away by a Galilean transformation [20] and, in turn, critical behavior is not affected by the global bias. Recently, a local hopping bias was introduced to the BAW [21] in such a manner that a particle prefers hopping toward the nearest particle. Since a particle is likely to get close to the nearest particle by the local bias, this form of interaction associated with the local bias is termed as attraction in Ref. [22]. Since hopping along any direction is equally likely on average, no macroscopic current is produced by the local bias. In this sense, the Galilean transformation cannot remove the local bias and, in turn, the local bias can be relevant in the renormalization-group (RG) sense. Indeed, it was shown that the local bias changes the critical behavior when the number m of offspring is even [21, 22].

Unlike a long-range jump (Lévy flight) introduced to models exhibiting an absorbing phase transition [23, 24], every particle still hops to one of its nearest-neighbor sites. In this sense, one may think of the local bias as

short-range interaction. This idea seems to have support because the BAW with an odd number of offspring is not affected by the local bias, while Lévy flight applied to DP models changes critical behavior [25–27]. However, it was argued that the local bias is irrelevant (in the RG sense) in the DP class not because the bias is short-ranged but because spontaneous annihilation ($A \rightarrow 0$) arising by combination of branching with pair annihilation ($A \rightarrow 2A \rightarrow 0$) removes the long-range nature of the local bias for odd m [22].

To reveal clearly the long-range nature of the local bias for the case of even number of offspring, Ref. [22] studied a modified model by introducing the range R of attraction. In the modified model, a particle is attracted to the nearest particle only if the distance between the two particles is not larger than R . When R is finite, the model with even m turned out to crossover to the DI class and the crossover behavior for large R is described by the exponent ϕ , which is found to be 1.39 ± 0.04 [22]. Therefore, it is concluded that the different critical behavior from the DI class in Ref. [21] is attributed to the long-range nature of the local bias.

Since long-range interaction usually entails continuously varying critical exponents [25–27], it is natural to ask if the local bias with appropriate generalization can trigger continuously varying exponents. The aim of this paper is to answer this question by studying such a generalized model that the strength of the local bias depends on the distance x to the nearest particle by a power-law function $x^{-\sigma}$. The case with $\sigma = 0$ will correspond to the model in Ref. [21]. We will investigate how the critical behavior changes with the value of σ .

The structure of this paper is as follows. In Sec. II, we define a model with a local bias. As explained above, the strength of the bias becomes a power-law function of distance to the nearest particle. We will call this model the branching annihilating random walks with long-range attraction (BAWL). In Sec. III, we present our simulation results, focusing on the critical decay exponent that is defined in Sec. II. We will also find σ_c that separates the DI critical behavior (for $\sigma \geq \sigma_c$) and non-DI critical be-

havior (for $\sigma < \sigma_c$). In Sec. IV, we discuss what happens if branching is biased. Section V summarizes the paper.

II. MODEL AND METHODS

The BAWL is defined on a one-dimensional lattice of size L with periodic boundary conditions. Each site i ($i = 1, 2, \dots, L$) is characterized by an occupation number a_i that takes either one or zero. If $a_i = 1$, we say that there is a particle at site i . If $a_i = 0$, we say that site i is vacant. For later purpose, we define r_i and l_i such that

$$\begin{aligned} r_i &= \min \{x | a_{i+x} = 1, x > 0\}, \\ l_i &= \min \{x | a_{i-x} = 1, x > 0\}, \end{aligned} \quad (1)$$

where we assume that site $j + L$ is identical to site j (periodic boundary condition). In words, r_i (l_i) is the distance from site i to the nearest particle on the right-hand (left-hand) side.

If there is a particle at site i ($a_i = 1$), it either hops to one of its nearest-neighbor sites with rate p (hopping event) or branches four offspring with rate $1 - p$ (branching event). In the hopping event, it hops to site $i \pm 1$ with probability q_{\pm} , where

$$q_{\pm} = \frac{1}{2} \pm \zeta x^{-\sigma}, \quad x = \min\{r_i, l_i\}, \quad \sigma \geq 0, \quad (2)$$

with ($0 \leq \epsilon \leq 0.5$)

$$\zeta = \begin{cases} \epsilon, & \text{if } r_i < l_i, \\ -\epsilon, & \text{if } r_i > l_i, \\ 0, & \text{if } r_i = l_i. \end{cases} \quad (3)$$

Notice that q_{\pm} mimics attraction by the nearest particle.

In the branching event, its four offspring are placed at sites $i - 2$, $i - 1$, $i + 1$, and $i + 2$ ($A \rightarrow 5A$). If a particle is to be placed at an already occupied site either by hopping or branching, these two particles are annihilated immediately ($2A \rightarrow 0$). We summarize the above dynamic rules as follows:

$$1_i a_{i+1} \rightarrow 0_i \bar{a}_{i+1} \text{ rate } pq_+, \quad (4a)$$

$$a_{i-i} 1_i \rightarrow \bar{a}_{i-1} 0_i \text{ rate } pq_-, \quad (4b)$$

$$1_i a_{i\pm 1} a_{i\pm 2} \rightarrow 1_i \bar{a}_{i\pm 1} \bar{a}_{i\pm 2} \text{ rate } 1 - p, \quad (4c)$$

where 1_i (0_i) means that a_i is one (zero) and $\bar{a}_j \equiv 1 - a_j$. We set $\epsilon = 0.1$ in simulations but other choice of nonzero ϵ does not change our conclusion.

The algorithm we have used to simulate the corresponding master equation to the rule (4) is as follows. Assume that there are N_t particles at time t . We choose one particle among N_t particles at random with equal probability. The chosen particle branches four offspring with probability $1 - p$ or hops toward (against) the nearest particle with probability pq_+ (pq_-), where q_{\pm} is defined in Eq. (2). If two particles happen to occupy a site, these

two particles are removed in no time. After the change, time increases by $1/N_t$.

The BAWL with $\sigma = 0$, which is identical to the model in Ref [21], does not belong to the DI class, while the BAWL under $\sigma \rightarrow \infty$ limit is equivalent to the model in Ref. [22] with $R = 1$ and, in turn, belongs to the DI class. Thus, there should be σ_c such that the BAWL with $\sigma \geq \sigma_c$ belongs to the DI class. In this paper, we will find σ_c and investigate the critical behavior for $\sigma < \sigma_c$.

We will study the average density ρ of occupied sites at time t defined as

$$\rho(t) = \frac{1}{L} \sum_{i=1}^L \langle a_i \rangle, \quad (5)$$

where $\langle \dots \rangle$ stands for average over all ensemble. The configuration with $a_i = 1$ for all i will be used as an initial condition in this paper.

At the critical point, $\rho(t)$ is expected to show a power-law behavior with a critical decay exponent δ such that

$$\rho(t) = At^{-\delta} [1 + Bt^{-\chi} + o(t^{-\chi})], \quad (6)$$

where $t^{-\chi}$ is the leading term of corrections to scaling, $o(x)$ stands for all terms that decrease faster than x as $x \rightarrow 0$, and A , B are constants. We will call χ the corrections-to-scaling exponent.

To find δ , we study an effective exponent $-\delta_e$ defined as

$$-\delta_e(t, b) \equiv \frac{\ln[\rho(t)/\rho(t/b)]}{\ln b}, \quad (7)$$

where b is a constant. At the critical point, the effective exponent in the long time limit should behave as

$$-\delta_e(t, b) \approx -\delta - B \frac{b^{\chi} - 1}{\ln b} t^{-\chi}. \quad (8)$$

From Eq. (8), it is obvious that at the critical point $-\delta_e$, when treated as a function of $t^{-\chi}$, should show a linear behavior for small $t^{-\chi}$. On the other hand, if the system is slightly off the critical point and is actually in the active (absorbing) phase, $-\delta_e$ should eventually veer up (down) as $t^{-\chi} \rightarrow 0$. Accordingly, we can find the critical point by observing how $-\delta_e$ behaves. Once we find the critical point, the critical decay exponent can be found by linear extrapolation of $-\delta_e$ vs $t^{-\chi}$ at the critical point.

To estimate δ accurately, information of χ is crucial. To find χ , we analyze a corrections-to-scaling function Q defined as [28, 29]

$$Q(t; b, \chi) = \frac{\ln \rho(t/b^2) + \ln \rho(t) - 2 \ln \rho(t/b)}{(b^{\chi} - 1)^2}, \quad (9)$$

whose asymptotic behavior at the critical point is $Q \sim Bt^{-\chi}$ regardless of the value of b if χ is correctly chosen. Notice that if B is positive (negative), $-\delta_e$ approaches $-\delta$ from below (above). In our system, we actually found that B is negative.

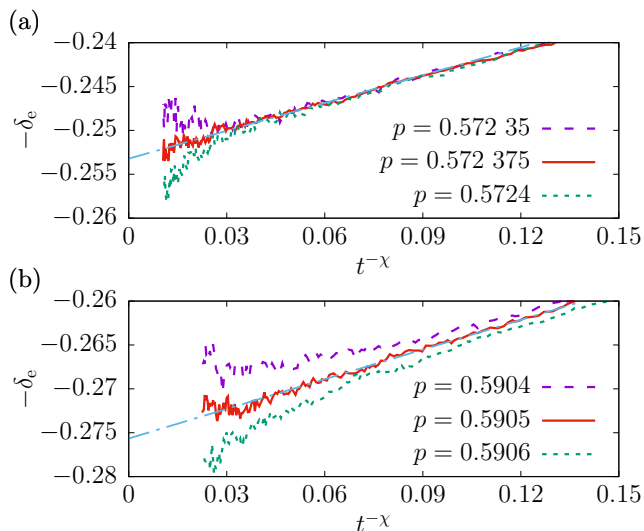


FIG. 1. Plots of $-\delta_e$ vs $t^{-\chi}$ (a) for $\sigma = 0.1$ at $p = 0.573\ 35$, $0.572\ 375$, 0.5724 (top to bottom) with $\chi = 0.3$ and $b = 16$ and (b) for $\sigma = 0.3$ at $p = 0.5904$, 0.5905 , 0.5906 (top to bottom) with $\chi = 0.25$ and $b = 16$. The (dot-dashed cyan) straight lines overlapping with the middle curves show the results of linear extrapolation for the critical decay exponent. Clearly, the critical decay exponent δ varies with σ .

For convenience, an i th measurement is performed at time T_i defined as

$$T_i = \begin{cases} i, & i \leq 40, \\ \lfloor 40 \times 2^{(i-40)/15} \rfloor, & 41 \leq i \leq 55, \\ 2T_{i-15}, & 56 \leq i, \end{cases} \quad (10)$$

where $\lfloor x \rfloor$ is the floor function (greatest integer not larger than x). With this choice of measurement time, we can set $b = 2^n$ ($n = 1, 2, \dots$) to analyze the effective exponent as well as the corrections-to-scaling function.

III. RESULTS

In this section, we present our simulation results for the critical decay exponent δ for various values of σ . To begin, we analyze the BAWL with $\sigma = 0.1$ and 0.3 . In simulations for these two cases, the system size is $L = 2^{23}$ and the maximum observation time is $T_{289} \approx 4 \times 10^6$. The number of independent runs is between 80 and 200. We first analyzed the corrections-to-scaling function Q and we found χ to be 0.3 and 0.25 for $\sigma = 0.1$ and 0.3 , respectively, see Supplemental Material [30]. In Fig. 1, we depict the effective exponent as a function of $t^{-\chi}$ for $\sigma = 0.1$ [Fig. 1(a)] and 0.3 [Fig. 1(b)] with $b = 16$.

Since middle curves in both panels show linear behaviors, while the other curves eventually veer up or down, we estimate the critical point as $p_c = 0.572\ 375(25)$ for $\sigma = 0.1$ and $p_c = 0.5905(1)$ for $\sigma = 0.3$, where the numbers in parentheses indicate uncertainty of the last digits.

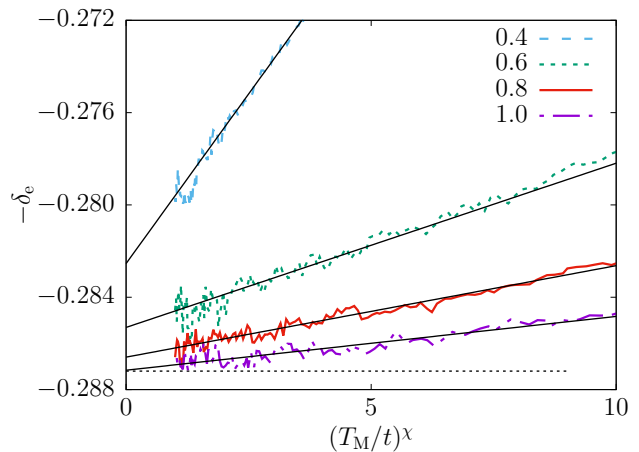


FIG. 2. Plots of $-\delta_e$ vs $(T_M/t)^\chi$ with $b = 32$ at the critical point for $\sigma = 0.4, 0.6, 0.8$ and 1 (top to bottom), where T_M is the maximum observation time. Here, $T_M = T_{289} \approx 4 \times 10^6$ for $\sigma = 0.4$ and $T_M = T_{309} \approx 10^7$ for other cases. Straight lines are results of linear extrapolation and the dotted horizontal line indicates the critical decay exponent of the DI class.

By linear extrapolation, we get $\delta = 0.2532(8)$ for $\sigma = 0.1$ and $0.276(1)$ for $\sigma = 0.3$. It is clear that δ does depend on σ , which is a typical feature of absorbing phase transitions with long-range jump [25–27, 31]. Once again we confirm the claim in Ref. [22] that the model with hopping bias in Ref. [21] does not belong to the DI class because of long-range interaction.

We have established that the critical decay exponent varies with σ . Now, we move on to finding σ_c . Recall that the BAWL with $\sigma \geq \sigma_c$ is supposed to belong to the DI class. We simulated the system of size $L = 2^{23}$ for various σ 's. As we have done in Fig. 1, we first found χ and p_c , then analyzed the effective exponent, see Supplemental Material [30].

Figure 2 depicts the resulting effective exponents at

TABLE I. Critical points (p_c), corrections-to-scaling exponents (χ), and critical decay exponents (δ) of the BAWL. The numbers in parentheses indicate uncertainty of the last digits.

σ	p_c	χ	δ
0 ^a	0.562 142(3)	0.3	0.2393(3)
0.1	0.572 375(25)	0.3	0.2532(8)
0.2	0.581 85(5)	0.3	0.2647(7)
0.3	0.5905(1)	0.25	0.276(1)
0.4	0.5983(1)	0.25	0.2828(8)
0.6	0.6112(1)	0.35	0.2855(5)
0.8	0.621 11(1)	0.4	0.2866(3)
1.0	0.628 75(5)	0.4	0.2872(4)

^a From Ref. [22].

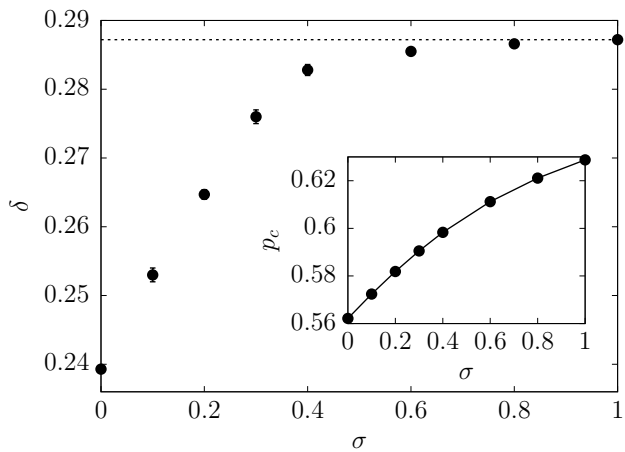


FIG. 3. Plot of δ vs σ . The critical decay exponent of the DI class is shown as a horizontal dotted line. The size of the error bar is comparable to the symbol size. (Inset) Plot of p_c vs σ . The line is for guides to the eyes.

the critical point for $\sigma = 0.4, 0.6, 0.8,$ and 1 against $(T_M/t)^\chi$, where T_M is the maximum observation time of each simulation for the corresponding parameter set. When $\sigma < 0.8$, the estimate of δ is clearly distinct from δ of the DI class that is shown as a dotted horizontal line in Fig. 2. For $\sigma = 1$, the critical decay exponent is hardly discernible from δ of the DI class, which seems to suggest $\sigma_c = 1$. Our preliminary simulations also showed that δ remains the same for $\sigma > 1$ (not shown here).

To affirm that δ for the case of $\sigma = 0.8$ is indeed larger than the critical decay exponent of the DI class, we extensively performed simulations for this case (800 independent runs are averaged). As shown in Fig. 2, our simulation results suggest that σ_c is indeed larger than 0.8, see Supplemental Material [30].

The values of p_c , χ , and δ for various σ 's [30] are summarized in Table I and in Fig. 3, we graphically show how δ and p_c depend on σ .

Now we will argue that σ_c is indeed one. Since the DI class is intimately related to the annihilation fixed point [13, 15], a necessary condition for a model to belong to the DI class is that the asymptotic behavior of density should be $t^{-0.5}$ in the absorbing phase. In this context, we will analyze how the density of the BAWL with $p = 1$ (without branching) behaves in the long time limit.

In the absorbing phase, the density approaches zero as $t \rightarrow \infty$. Hence, the asymptotic behavior of the density for the BAWL with $p = 1$ can be understood by studying a random walk model with an attracting center at the origin. In this random walk model, a walker located at site n ($n > 0$) hops to the right with rate $(1 - vn^{-\sigma})/2$ and to the left with rate $(1 + vn^{-\sigma})/2$. Now we will find the mean first-passage time to the origin, once it starts from site m . It is convenient to regard the origin as an absorbing wall.

The analysis starts from writing down the master equa-

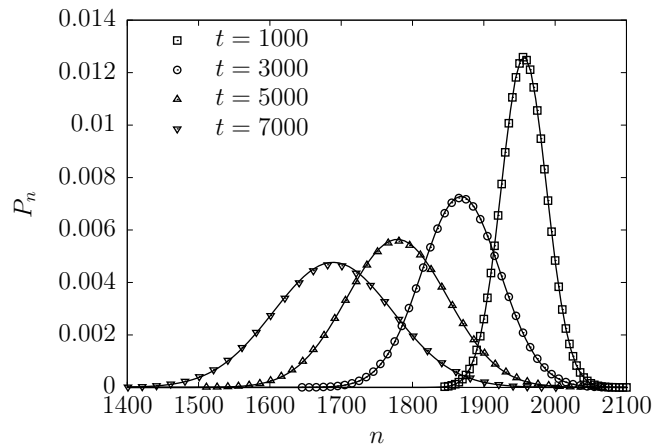


FIG. 4. Plots of $P_n(t)$ vs n at $t = 1000, 3000, 5000,$ and 7000 (right to left). Initial position is set $m = 2000$. Solid curves depicts the approximate solution (17).

tion ($n \geq 1$)

$$\frac{\partial}{\partial t} P_n(t) = -P_n(t) + \frac{1 + v(n+1)^{-\sigma}}{2} P_{n+1}(t) + \frac{1 - v(n-1)^{-\sigma}}{2} (1 - \delta_{n,1}) P_{n-1}(t), \quad (11)$$

$$\frac{\partial}{\partial t} P_0(t) = \frac{1+v}{2} P_1(t), \quad (12)$$

where $P_n(t)$ is the probability that the walker is at site n at time t . For $n \geq 2$, we rewrite Eq. (11) as

$$\frac{\partial}{\partial t} P_n(t) = -\partial_n [-vn^{-\sigma} P_n(t)] + \frac{1}{2} \partial_n^2 P_n(t), \quad (13)$$

where $\partial_n f(n) \equiv [f(n+1) - f(n-1)]/2$ and $\partial_n^2 f(n) \equiv f(n+1) + f(n-1) - 2f(n)$. Taking (naive) continuum limit, we get a Fokker-Planck equation (n is now a continuous variable)

$$\frac{\partial}{\partial t} P(n, t) = -\frac{\partial}{\partial n} [-vn^{-\sigma} P(n, t)] + \frac{1}{2} \frac{\partial^2}{\partial n^2} P(n, t), \quad (14)$$

which is equivalent to the Langevin equation

$$\dot{n} = -vn^{-\sigma} + \xi, \quad (15)$$

where ξ is the white noise with zero mean and unit variance.

Using a mean-field-like approximation $\langle n^{-\sigma} \rangle \approx \langle n \rangle^{-\sigma}$, where $\langle \dots \rangle$ is the average over noise, we get

$$\langle \dot{n} \rangle \approx -\frac{v}{\langle n \rangle^\sigma} \Rightarrow \langle n \rangle \approx m \left[1 - \frac{(1+\sigma)vt}{m^{1+\sigma}} \right]^{1/(1+\sigma)}, \quad (16)$$

where m is the initial position of the walker. If we further assume that the white noise makes P_n be a Gaussian with variance t , we arrive at

$$P_n(t) \approx \frac{1}{\sqrt{2\pi t}} \exp \left[-\frac{(n - \langle n \rangle)^2}{2t} \right], \quad (17)$$

for sufficiently large n (and m).

To check how good the approximation is, we performed Monte Carlo simulations for the continuous time master equation (11) with $\sigma = 0.2$, $v = 0.2$, and $m = 2000$. In Fig. 4, we show $P_n(t)$ at $t = 1000, 3000, 5000, 7000$ together with Eq. (17). Our approximation is in an excellent agreement with numerical (exact) result.

If $\sigma < 1$, the mean first-passage time τ to the origin is obtained by $\langle n \rangle = 0$, which gives $\tau \sim m^{1+\sigma}$. On the other hand, if $\sigma > 1$, the spreading by fluctuation is faster than the deterministic motion. Accordingly, time τ to arrive at the origin is dominated by diffusion, which gives $\tau \sim m^2$. If we write $\tau \sim m^z$, we find

$$z = \begin{cases} 1 + \sigma, & \sigma < 1 \\ 2, & \sigma \geq 1. \end{cases} \quad (18)$$

From Eq. (18) and the scaling argument for the pair annihilation dynamics [32, 33], we predict that the long time behavior of the density is $t^{-\alpha}$ with

$$\alpha = 1/z = \begin{cases} 1/(1 + \sigma), & \text{if } \sigma < 1, \\ 1/2, & \text{if } \sigma \geq 1. \end{cases} \quad (19)$$

To confirm the anticipation, we simulated the BAWL with $\epsilon = 0.1$ and $p = 1$ for various σ 's. We present the behavior of effective exponent $-\alpha_e$ for $\sigma = 0.2, 0.6$, and 1 in Fig. 5, which shows an excellent agreement with the analytic argument.

From the above analysis, the BAWL with $\sigma < 1$ should not belong to the DI class, as we have seen in Fig. 2. Since the BAWL with $\sigma = 1$ belongs to the DI class as shown in Fig. 2, we conclude that the upper bound σ_c is indeed 1

IV. DISCUSSION: BRANCHING BIAS

We have shown that the local hopping bias due to long-range attraction with decreasing strength as $x^{-\sigma}$ continuously changes the critical decay exponent of the BAWL when $\sigma \leq 1$. Now, we would like to ask which one determines the critical behavior, *hopping* bias or *bias in itself*. To answer this question, we modify the BAWL in such a way that hopping is symmetric but branching is biased. To be concrete, we will now investigate a model with dynamics

$$1_i a_{i\pm 1} \rightarrow 0_i \bar{a}_{i\pm 1} \quad \text{rate } p/2, \quad (20a)$$

$$1_i \prod_{k=1}^4 a_{i+k} \rightarrow 1_i \prod_{k=1}^4 \bar{a}_{i+k} \quad \text{rate } (1-p)q_+, \quad (20b)$$

$$1_i \prod_{k=1}^4 a_{i-k} \rightarrow 1_i \prod_{k=1}^4 \bar{a}_{i-k} \quad \text{rate } (1-p)q_-, \quad (20c)$$

where q_{\pm} is the same as in Eq. (2) and we use the same notation as in Eq. (4).

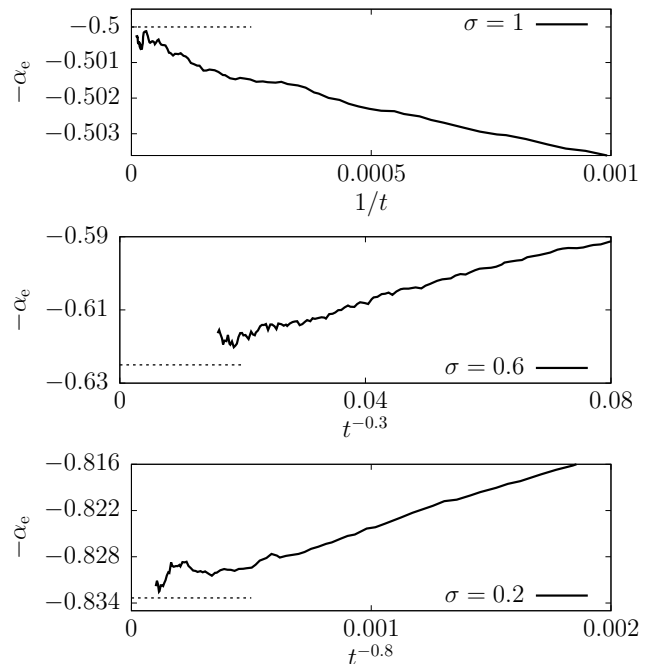


FIG. 5. Plots of $-\alpha_e$ vs $t^{-\chi}$ for $\sigma = 0.2$ ($\chi = 0.8$: bottom), $\sigma = 0.6$ ($\chi = 0.3$: middle), and $\sigma = 1$ ($\chi = 1$: top). Dotted line segments indicate the anticipated value of $-\alpha$ from Eq. (19)

Before presenting simulation results, let us ponder on what would happen in this modified model. The driven pair contact process with diffusion (DPCPD) [20] would be a good starting point for our discussion. In the DPCPD, though it has global bias, only presence of bias is an important factor to determine the universality class, as it is immaterial whether hopping or branching is biased [34]. In this regard, one would conclude that *bias in itself* is relevant (in the RG sense) and that the critical behavior of the BAWL would not be affected by to which dynamic process the local bias is applied. However, the DPCPD should be considered a system with two independent fields and both the hopping bias and the branching bias in the DPCPD generates a relative bias between the two fields [20, 35]. Since the BAW is described by a single field [13, 15], the discussion about the DPCPD would not give a clear answer to our question.

In the mean time, one may easily come up with an argument that only *hopping* bias is relevant, because the density of the modified model with $p = 1$ (trivially) behaves as $t^{-0.5}$ for any σ . This should be compared with the discussion in Sec. III, based on the analysis of the BAWL with $p = 1$. However, this argument has a serious flaw; the dynamics at $p = 1$ may not represent the absorbing phase of the modified model. An example in this context is the BAW with one offspring (BAW₁). As in the BAWL, let us denote the branching rate of the BAW₁ by $1-p$. If $p = 1$, the density (again trivially) decays as $t^{-0.5}$. If branching rate is turned on, however, a

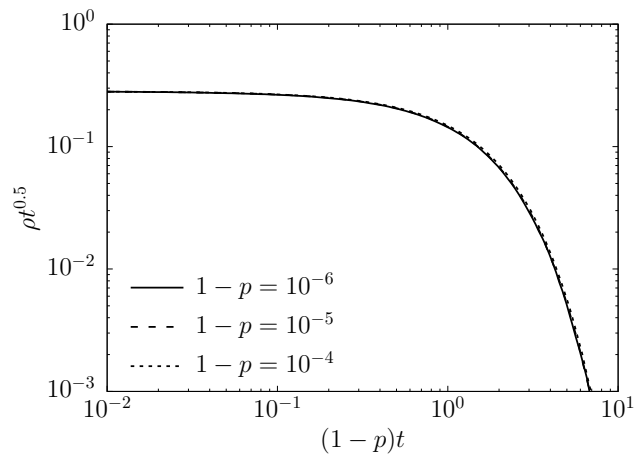


FIG. 6. Scaling-collapse plot of $\rho t^{0.5}$ vs $(1-p)t$ of the BAW_1 for $1-p = 10^{-4}$, 10^{-5} , and 10^{-6} on a double-logarithmic scale. As anticipated by Eq. (21), curves for different p 's are hardly discernible.

spontaneous annihilation of a single particle by the chain of reactions $A \rightarrow 2A \rightarrow 0$ can occur, which results in an exponential density decay. That is, the BAW_1 with $p = 1$ cannot capture the main feature (exponential density decay in this example) of its absorbing phase.

Actually, the behavior of the BAW_1 around $p = 1$ can be described by a scaling function

$$\rho(t) = t^{-0.5} F[(1-p)t], \quad (21)$$

where $F(x)$ is expected to decrease exponentially for large x . The reason why $(1-p)t$ should be a single scaling parameter is clear. The spontaneous annihilation can be crucial only when substantial amount of branching events have occurred, which is expected if time elapses more than $1/(1-p)$. In Fig. 6, we show scaling collapse of the BAW_1 for p close to 1, which confirms the scaling ansatz (21). Here, the system size is 2^{25} and average over 8 independent runs for each parameter is taken. As the example of the BAW_1 reveals, it is possible that $p = 1$ of the modified model is in a sense a singular point and that the modified model in the absorbing phase does not exhibit $t^{-0.5}$ behavior for small σ .

To obtain the answer, we now resort to Monte Carlo simulations. Using systems of size $L = 2^{24}$, we performed simulations for $\epsilon = 0.5$ and $p = 0.8$. To reduce statistical error, we performed 40 independent runs for each parameter set. Figure 7 shows the behavior of the density for $\sigma = 0, 0.2, 0.6$, and 1 on a double logarithmic scale. Just like the BAWL with $p = 1$, the density decays as $t^{-\alpha}$ with α in Eq. (19). Hence, we expect that the critical behavior is the same regardless of whether hopping or branching is biased. We have checked this anticipation by simulations and our preliminary simulations for $\sigma = 0$ indeed show that the critical behavior of the modified model is the same as the BAWL (details not shown here). This also indirectly confirms that the BAWL with $p = 1$ correctly

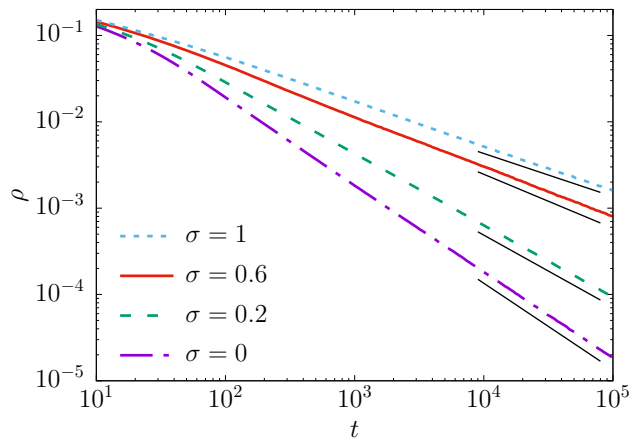


FIG. 7. Double-logarithmic plots of ρ vs t of the model with dynamic rules (20) for $\sigma = 0, 0.2, 0.6$, and 1 (bottom to top). Here, we set $p = 0.8$ for all cases. For guides to the eyes, we also depict a line segment with slope $-1/(1+\sigma)$ right below each curve.

represents the behavior in the absorbing phase. To conclude this section, we have shown that the presence of the local bias due to long-range attraction is enough to exhibit non-DI critical phenomena, irrespective of which dynamic process the local bias is applied.

V. SUMMARY

To summarize, we studied the branching annihilating random walks with long-range attraction (BAWL). The long-range attraction has a power-law feature with exponent σ ; see Eq. (2). We investigated the critical decay exponent δ that describes how the density behaves with time at the critical point. We first numerically found that δ varies continuously with σ for $\sigma < 1$ and is the same as the critical decay exponent of the directed Ising universality class for $\sigma \geq 1$. By the analysis of a random walk with an attracting center at the origin together with Monte Carlo simulations for the BAWL with $p = 1$, we argued that σ_c should be 1.

We also studied the modified model in which offspring prefer being placed toward the nearest particle but hopping is now unbiased. We found that the absorbing phase of the modified model shows the same asymptotic behavior of the BAWL for the same value of σ . Therefore, we concluded that it is immaterial which dynamic process, hopping or branching, is biased by the long-range attraction.

ACKNOWLEDGMENTS

This work was supported by the Basic Science Research Program through the National Research Foundation of Korea (NRF) funded by the Ministry of Science

and ICT (Grant No. 2017R1D1A1B03034878). The author furthermore thanks the Regional Computing Cen-

ter of the University of Cologne (RRZK) for providing computing time on the DFG-funded High Performance Computing (HPC) system CHEOPS.

-
- [1] H. Takayasu and A. Y. Tretyakov, Extinction, survival, and dynamical phase transition of branching annihilating random walk, *Phys. Rev. Lett.* **68**, 3060 (1992).
- [2] I. Jensen, Critical exponents for branching annihilating random walks with an even number of offspring, *Phys. Rev. E* **50**, 3623 (1994).
- [3] D. Zhong and D. ben Avraham, Universality class of two-offspring branching annihilating random walks, *Phys. Lett.* **209**, 333 (1995).
- [4] S. Kwon and H. Park, Reentrant phase diagram of branching annihilating random walks with one and two offspring, *Phys. Rev. E* **52**, 5955 (1995).
- [5] S. R. Broadbent and J. M. Hammersley, Percolation processes: I. Crystals and mazes, *Math. Proc. Camb. Phil. Soc.* **53**, 629 (1957).
- [6] P. Grassberger and A. de la Torre, Reggeon field-theory (Schlöggl's 1st model) on a lattice - Monte-Carlo calculations of critical behavior, *Ann. Phys. (NY)* **122**, 373 (1979).
- [7] J. L. Cardy and R. L. Sugar, Directed percolation and Reggeon field theory, *J. Phys. A* **13**, L423 (1980).
- [8] H.-K. Janssen, On the nonequilibrium phase transition in reaction-diffusion systems with an absorbing stationary state, *Z. Phys. B* **42**, 151 (1981).
- [9] P. Grassberger, On phase transitions in Schlöggl's second model, *Z. Phys. B* **47**, 365 (1982).
- [10] P. Grassberger, F. Krause, and T. von der Twer, A new type of kinetic critical phenomenon, *J. Phys. A* **17**, L105 (1984).
- [11] M. H. Kim and H. Park, Critical behavior of an interacting monomer-dimer model, *Phys. Rev. Lett.* **73**, 2579 (1994).
- [12] N. Menyhárd and G. Ódor, Phase transitions and critical behaviour in one-dimensional non-equilibrium kinetic Ising models with branching annihilating random walk of kinks, *J. Phys. A: Math. Gen.* **29**, 7739 (1996).
- [13] J. Cardy and U. C. Täuber, Theory of branching and annihilating random walks, *Phys. Rev. Lett.* **77**, 4780 (1996).
- [14] H. Hinrichsen, Stochastic lattice models with several absorbing states, *Phys. Rev. E* **55**, 219 (1997).
- [15] L. Canet, H. Chaté, B. Delamotte, I. Dornic, and M. A. Muñoz, Nonperturbative fixed point in a nonequilibrium phase transition, *Phys. Rev. Lett.* **95**, 100601 (2005).
- [16] O. Al Hammal, H. Chaté, I. Dornic, and M. A. Muñoz, Langevin description of critical phenomena with two symmetric absorbing states, *Phys. Rev. Lett.* **94**, 230601 (2005).
- [17] H. Hinrichsen, Non-equilibrium critical phenomena and phase transitions into absorbing states, *Adv. Phys.* **49**, 815 (2000).
- [18] G. Ódor, Universality classes in nonequilibrium lattice systems, *Rev. Mod. Phys.* **76**, 663 (2004).
- [19] M. Henkel, H. Hinrichsen, and S. Lübeck, *Non-Equilibrium Phase Transitions: Absorbing Phase Transitions* (Springer, The Netherlands, 2008).
- [20] S.-C. Park and H. Park, Driven pair contact process with diffusion, *Phys. Rev. Lett.* **94**, 065701 (2005).
- [21] B. Daga and P. Ray, Universality classes of absorbing phase transitions in generic branching-annihilating particle systems with nearest-neighbor bias, *Phys. Rev. E* **99**, 032104 (2019).
- [22] S.-C. Park, Crossover behaviors in branching annihilating attracting walk, *Phys. Rev. E* **101**, 052103 (2020).
- [23] D. Mollison, Spatial contact models for ecological and epidemic spread, *J. R. Statist. Soc. B* **39**, 283 (1977).
- [24] P. Grassberger, Spreading of epidemic processes leading to fractal structures, in *Fractals in Physics*, edited by E. Tosatti and L. Pietrelli (North-Holland, Amsterdam, 1986) pp. 273–278.
- [25] H. K. Janssen, K. Oerding, F. van Wijland, and H. J. Hilhorst, Lévy-flight spreading of epidemic processes leading to percolating clusters, *Eur. Phys. J. B* **7**, 137 (1999).
- [26] H. Hinrichsen and M. Howard, A model for anomalous directed percolation, *Eur. Phys. J. B* **7**, 635 (1999).
- [27] H.-K. Janssen and O. Stenull, Field theory of directed percolation with long-range spreading, *Phys. Rev. E* **78**, 061117 (2008).
- [28] S.-C. Park, High-precision estimate of the critical exponents for the directed Ising universality class, *J. Korean Phys. Soc.* **62**, 469 (2013).
- [29] S.-C. Park, Critical decay exponent of the pair contact process with diffusion, *Phys. Rev. E* **90**, 052115 (2014).
- [30] See Supplemental Material at <http://link.aps.org/supplemental/10.1103/PhysRevE.101.052125> for details of numerical analysis.
- [31] D. Vernon and M. Howard, Branching and annihilating Lévy flights, *Phys. Rev. E* **63**, 041116 (2001).
- [32] K. Kang and S. Redner, Scaling approach for the kinetics of recombination processes, *Phys. Rev. Lett.* **52**, 955 (1984).
- [33] K. Kang and S. Redner, Fluctuation-dominated kinetics in diffusion-controlled reactions, *Phys. Rev. A* **32**, 435 (1985).
- [34] S.-C. Park and H. Park, Crossover from the parity-conserving pair contact process with diffusion to other universality classes, *Phys. Rev. E* **79**, 051130 (2009).
- [35] S.-C. Park and H. Park, Nonequilibrium phase transitions into absorbing states, *Eur. Phys. J. B* **64**, 415 (2008).

Supplemental Material for “Branching Annihilating Random Walks with Long-Range Attraction in One Dimension”

Su-Chan Park (박수찬)

The Catholic University of Korea, Bucheon 14662, Republic of Korea

In this Supplemental Material, we present details of numerical analyses for the corrections-to-scaling function Q and the effective exponent δ_e that are defined in the main text. Since the coefficients of Q for all cases are found to be negative, we depict $-Q$ as a function of t on a double logarithmic scale. We estimate χ by observing that the asymptotic behavior of Q does not depend on b . We also explain how we find the critical point from the effective exponent.

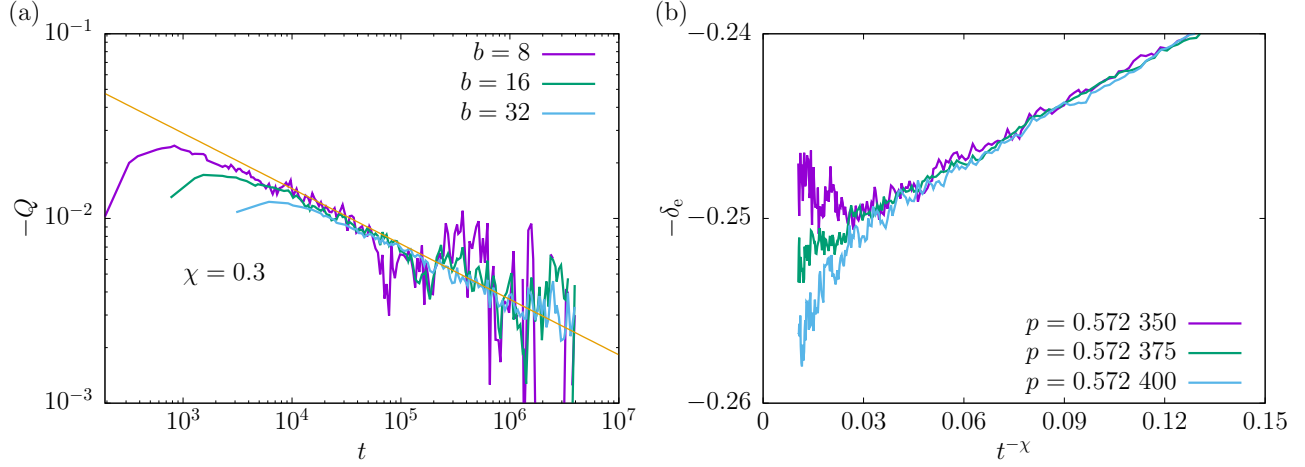


Fig. S1. $\sigma = 0.1$. (a) Double-logarithmic plots of $-Q$ vs t at the critical point with $b = 8, 16,$ and 32 . The estimated χ is explicitly written. We also depicts $t^{-\chi}$ for guides to the eyes. (b) Plots of $-\delta_e$ vs $t^{-\chi}$ around the critical point with $b = 16$. Since the middle curve shows the best linear behavior, we conclude $p_c = 0.572\ 375(25)$.

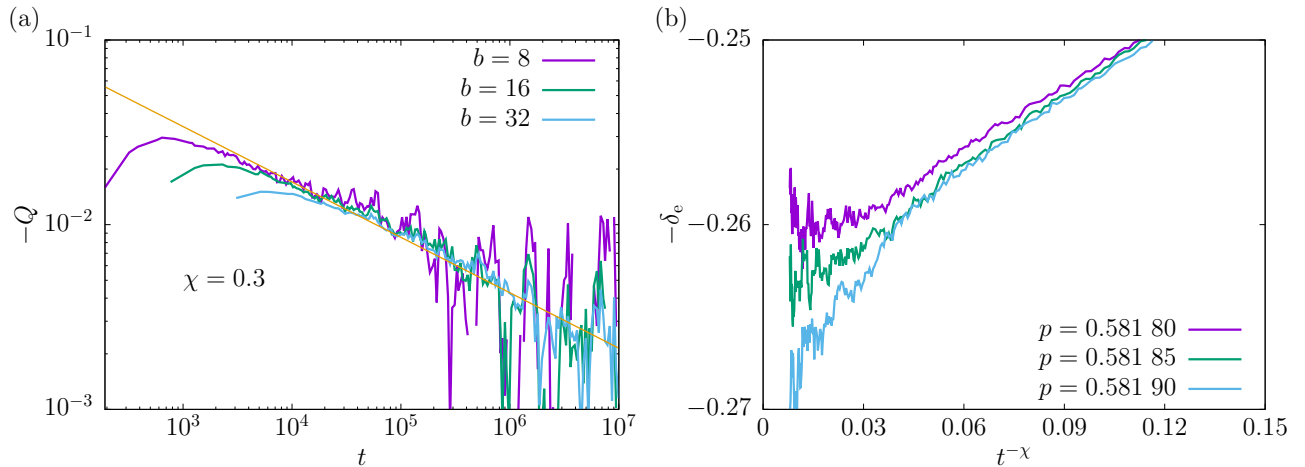


Fig. S2. $\sigma = 0.2$. (a) Double-logarithmic plots of $-Q$ vs t at the critical point with $b = 8, 16,$ and 32 . The estimated χ is explicitly written. We also depicts $t^{-\chi}$ for guides to the eyes. (b) Plots of $-\delta_e$ vs $t^{-\chi}$ around the critical point with $b = 16$. Since the middle curve shows the best linear behavior, we conclude $p_c = 0.581\ 85(5)$.

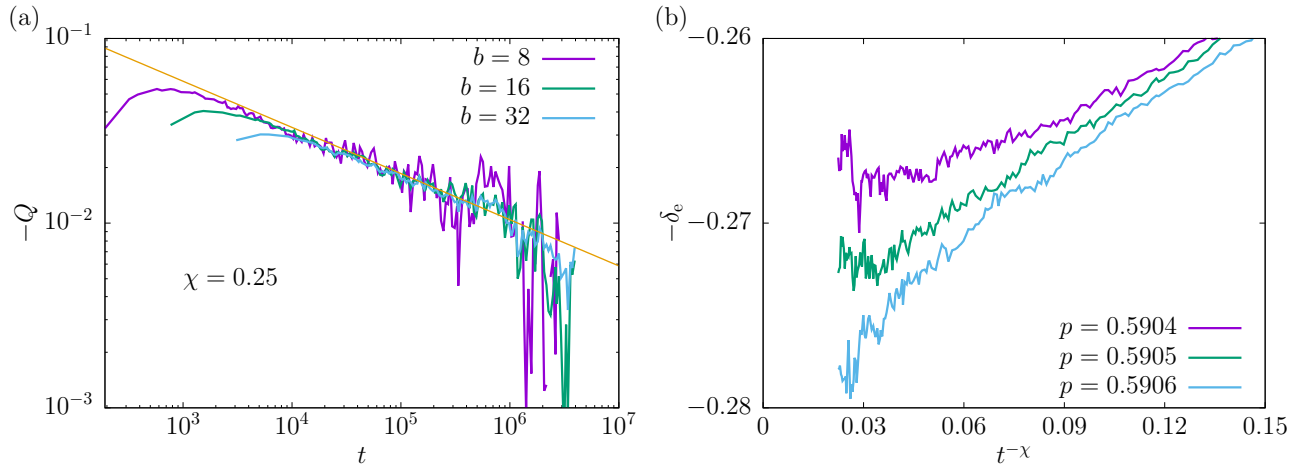


Fig. S3. $\sigma = 0.3$. (a) Double-logarithmic plots of $-Q$ vs t at the critical point with $b = 8, 16$, and 32 . The estimated χ is explicitly written. We also depicts $t^{-\chi}$ for guides to the eyes. (b) Plots of $-\delta_e$ vs $t^{-\chi}$ around the critical point with $b = 16$. Since the middle curve shows the best linear behavior, we conclude $p_c = 0.5905(1)$.

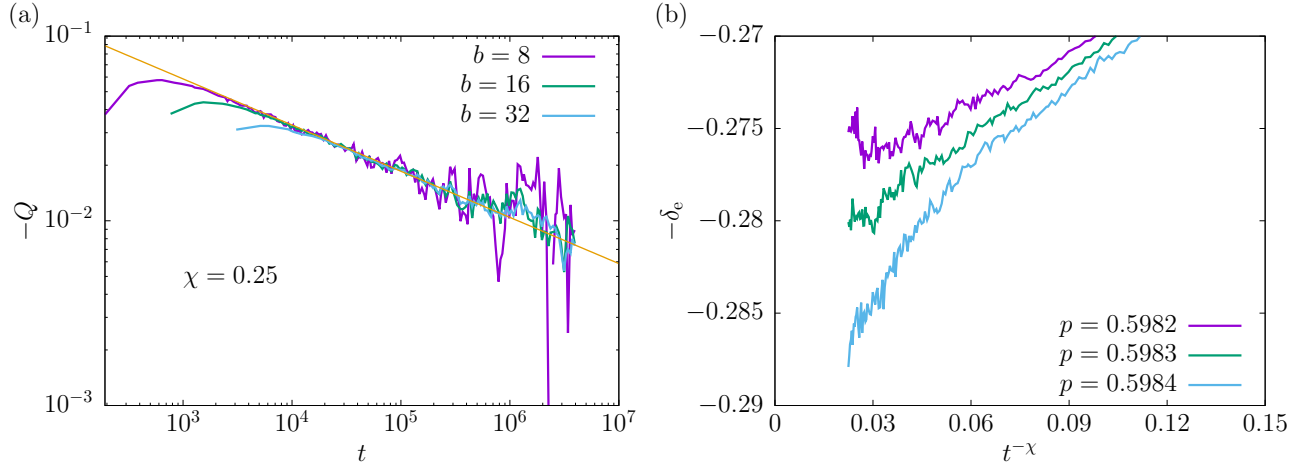


Fig. S4. $\sigma = 0.4$. (a) Double-logarithmic plots of $-Q$ vs t at the critical point with $b = 8, 16$, and 32 . The estimated χ is explicitly written. We also depicts $t^{-\chi}$ for guides to the eyes. (b) Plots of $-\delta_e$ vs $t^{-\chi}$ around the critical point with $b = 16$. Since the middle curve shows the best linear behavior, we conclude $p_c = 0.5983(1)$.

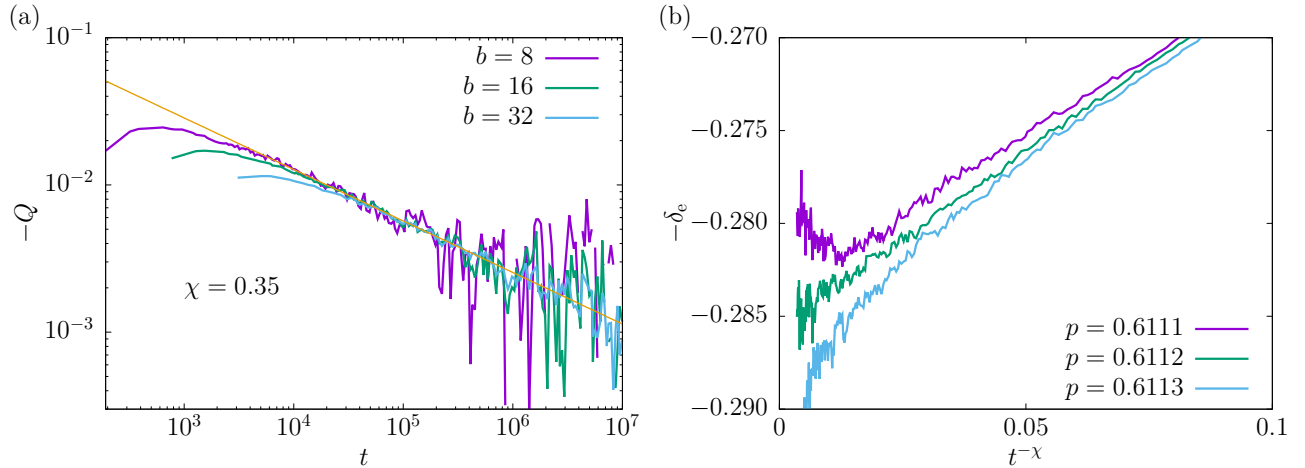


Fig. S5. $\sigma = 0.6$. (a) Double-logarithmic plots of $-Q$ vs t at the critical point with $b = 8, 16$, and 32 . The estimated χ is explicitly written. We also depicts $t^{-\chi}$ for guides to the eyes. (b) Plots of $-\delta_e$ vs $t^{-\chi}$ around the critical point with $b = 16$. Since the middle curve shows the best linear behavior, we conclude $p_c = 0.6112(1)$.

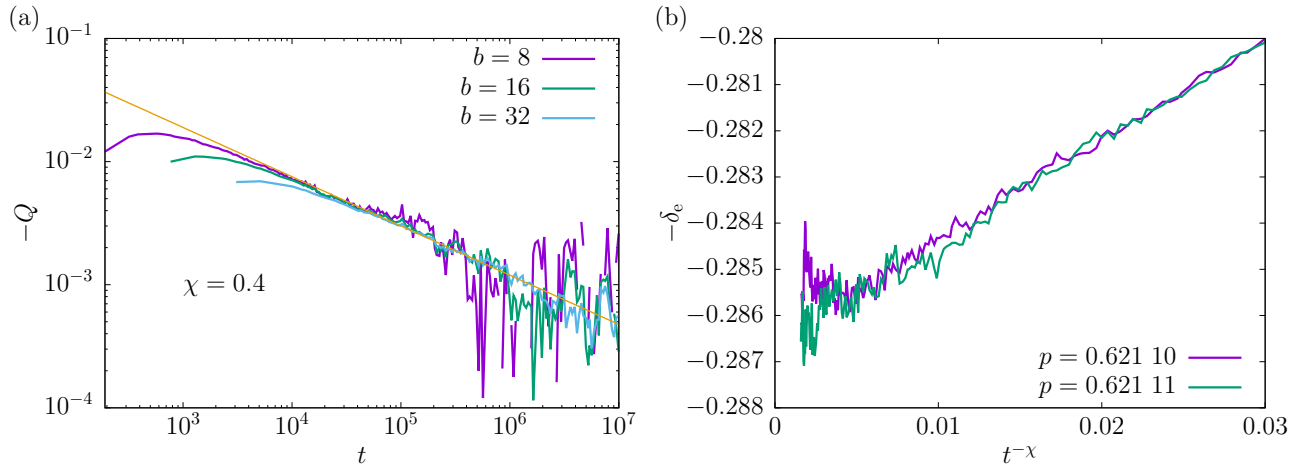


Fig. S6. $\sigma = 0.8$. (a) Double-logarithmic plots of $-Q$ vs t at the critical point with $b = 8, 16$, and 32 . The estimated χ is explicitly written. We also depicts $t^{-\chi}$ for guides to the eyes. (b) Plots of $-\delta_e$ vs $t^{-\chi}$ around the critical point with $b = 16$. Since the bottom curve shows the best linear behavior, we conclude $p_c = 0.621\ 11(1)$.

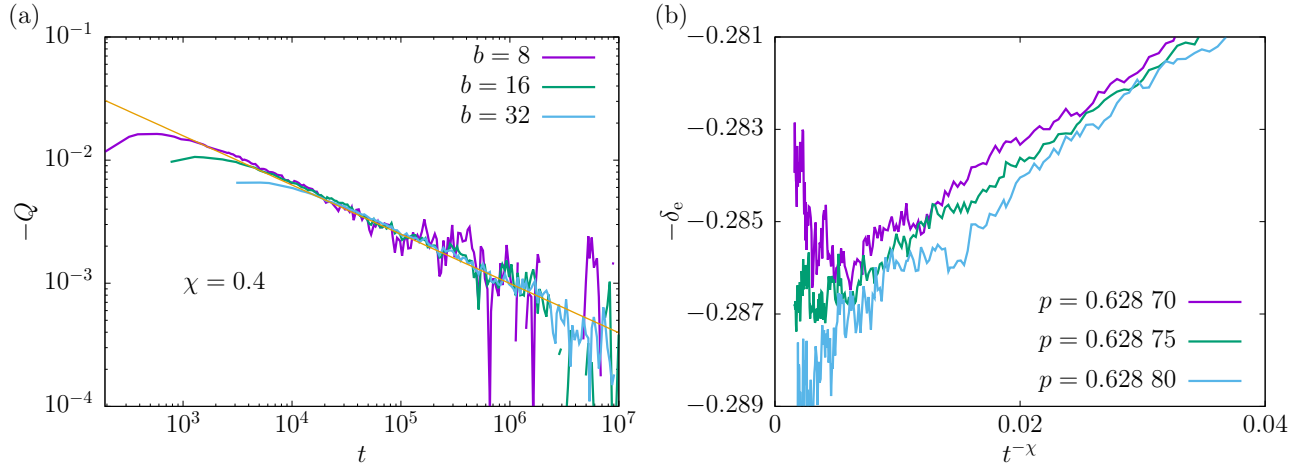


Fig. S7. $\sigma = 1$. (a) Double-logarithmic plots of $-Q$ vs t at the critical point with $b = 8, 16$, and 32 . The estimated χ is explicitly written. We also depicts $t^{-\chi}$ for guides to the eyes. (b) Plots of $-\delta_e$ vs $t^{-\chi}$ around the critical point with $b = 16$. Since the middle curve shows the best linear behavior, we conclude $p_c = 0.628\ 75(5)$.